A Model-Based Machine Learning Approach to Probing Autonomic Regulation from Nonstationary Vital-Sign Time Series

Li-wei H. Lehman[1†], Roger G. Mark[1], and Shamim Nemati[2]
Massachusetts Institute of Technology, Cambridge, MA
[2] Emory University, Atlanta, GA

***Abstract*—Physiological variables, such as heart rate (HR), blood pressure (BP) and respiration (RESP), are tightly regulated and coupled under healthy conditions, and a break-down in the coupling has been associated with aging and disease. We present an approach that incorporates physiological modeling within a switching linear dynamical systems (SLDS) framework to assess the various functional components of the autonomic regulation through transfer function analysis of nonstationary multivariate time series of vital signs. We validate our proposed SLDS-based transfer function analysis technique in automatically capturing (i) changes in baroreflex gain due to postural changes in a tilt-table study including 10 subjects, and (ii) the effect of aging on the autonomic control using HR/RESP recordings from 40 healthy adults. Next, using HR/BP time series of over 450 adult ICU patients, we show that our technique can be used to reveal coupling changes associated with severe sepsis (AUC=0.74, sensitivity=0.74, specificity=0.60). Our findings indicate that reduced HR/BP coupling is significantly associated with severe sepsis even after adjusting for clinical interventions (P<=0.001). These results demonstrate the utility of our approach in phenotyping complex vital-sign dynamics, and in providing mechanistic hypotheses in terms of break-down of autoregulatory systems under healthy and disease conditions.**

***Index Terms*—Switching Linear Dynamical Systems, Physiological Control Systems, RSA, Baroreflex, HRV.**

I. Introduction

Physiological control systems achieve autoregulation through feedback among multiple physiological variables, with the objective of maintaining homeostasis in the presence of internal and external disturbances. The resulting time series of vital signs, such as heart rate (HR), blood pressure (BP), and respiration (RESP), can exhibit complex variability patterns over multiple time scales [1], [2], [3]. A goal of physiological signal analysis is to quantitatively track the evolving dynamics and interactions among multivariate vital-sign signals to probe the underlying physiological control systems, and derive mechanistic understanding of how vital-sign dynamics are altered in health and disease. Spectral and non-linear dynamics of heart rate variability (HRV) [4], [5], [6], [7] and multivariate cardiovascular coupling analyses [8], [9], [10] have been used for assessment of autoregulation. HRV analysis has revealed several spectral peaks which have been attributed to the sympathetic, parasympathetic, renin-angiotensin, and thermoregulatory mechanisms [11]. For instance, high-frequency (HF) oscillations in HR time series have been shown to mostly reflect parasympathetic modulations; specifically, HF oscillations ($\sim$0.15 to 0.4 Hz) at the respiratory frequency are commonly referred to as the *respiratory sinus arrhythmia* (RSA). Low-frequency (LF) oscillations ($\sim$0.04 to 0.15) [1] of HR time series reflect mostly sympathetic modulations. The very low-frequency (VLF) components ($\sim$0.003 to 0.04 Hz) [1] have been postulated to reflect thermoregulation as well as low-frequency oscillations in breathing [12]. The LF/HF ratio of the HR spectrum has been used as an index of sympathovagal activation; increased LF/HF ratio may be due to sympathetic modulations [1], [5] or slow respiration. Moreover, cross-spectral techniques have been developed to investigate the frequency-dependent relationships between oscillations in HR, BP, and RESP [13], [14]. Nonlinear model identification techniques, such as the nonlinear autoregressive models, have been adopted to study coupling of multivariate cardiovascular time series [15], [16].

However, application of spectral, cross-spectral, and nonlinear coupling analyses to critical care patients has been limited due to the *nonstationary* characteristics of the underlying time series, recording noise and artifacts, as well as, the difficulty of accounting for clinical context and interventions. Traditional techniques assume time series stationarity, and cannot properly model transient phenomena or track evolving dynamics effectively. More recently, time varying autoregressive and point process based techniques have been developed to quantify the relationship between multiple variables in *nonstationary* physiological time series and to extract spectral indices of autonomic control [17], [18]. However, these techniques model each time series individually, and as a result, it is not clear how they can be applied to identify phenotypic dynamic behaviors exhibited across a patient cohort.

In this work, we present a switching linear dynamical systems (SLDS) approach to study various functional components of autonomic regulation through transfer function analysis of vital-sign time series. In particular, we incorporate a physiological model of cardiovascular control within a switching vector autoregressive (SVAR) processes framework [19] to characterize autonomic regulation, and model the evolving vital-sign dynamics of a patient cohort in terms of a collection

† Corresponding Author: LH Lehman (lilehman@mit.edu).
To appear in IEEE Journal of Biomedical and Health Informatics, Accepted November 21, 2016. doi:10.1109/JBHI.2016.2636808.

of simpler linear dynamical systems (or modes). Each such dynamic mode can be used to derive both indices of monovariate variability (similar to HRV analysis) and directional transfer functions of multivariate time series, and thereby capture autoregulatory changes in response to internal (such as onset of infection) and external perturbations (such as postural changes).

Our technique allows for simultaneous learning of a shared library of dynamic modes and segmentation of individual time series into regimes of approximate stationary dynamics. By jointly modeling multiple time series from a patient cohort in a probabilistic framework, our approach identifies shared dynamic behaviors across multiple multivariate nonstationary time series, and enables association analysis and interpretation of distinct dynamic behaviors in a given clinical context. We show that given a learned SVAR model from a collection of time series, the autoregressive coefficients corresponding to each of the discovered dynamic modes can be used to capture the spectral characteristics and oscillations that are present within the individual time series, and therefore can be used to extract useful indices of HR and BP variability. Moreover, given multivariate time series of vital signs, one can use the learned dynamics to derive the coupling strength among multiple observed time series and the directional transfer functions of the system (e.g., *baroreflex* control of beat-by-beat HR and BP) [20].

The underlying premise of our approach is that although autonomic regulation includes nonlinear components and is likely subject to non-Gaussian physiological noise, the system behavior can be described in terms of a convex combination of J linear dynamical systems (or *modes*), where the combination weights are given by the probability of belonging to each mode. This is known as *soft-switching* within the machine learning literature [21], and has been applied to modeling and tracking the complex dynamics of maneuvering airplanes [22]. For example, if the two basic dynamical modes of an airplane trajectory cover horizontal and vertical motion, one can represent turns using a convex combination of the individual modes [21]. In this work, we used an SLDS based soft-switching approach to model physiological time series, and introduce the concept of mode proportioned power spectra and transfer functions, i.e, weighting the contribution of power and gain from the j-th dynamic mode at time t according to the posterior probability that the observations at time t were generated by the j-th mode.

Our previous work based on the SVAR framework focused on using dynamics of blood pressure and heart rate time series from ICU patients to predict hospital mortality [19]. In contrast, our current work is focused on deriving mechanistic understanding of the observed vital-sign dynamics in terms of the directional influences among the interacting variables at specific frequency bands, and studying how oscillations and directional couplings are altered in diseased states.

The rest of the paper is organized as follows: we validate the proposed technique in tracking the changes in baroreflex gains from a laboratory study of subjects undergoing a tilt-table test, where the timing of occurrences of the different dynamics and the sharing of the dynamics across multiple time series/subjects were known a priori. Next, we validate the ability of our approach in capturing the influence of respiration on heart rate (or the RSA) using the Fantasia dataset, consisting of 20 young (21-34 years) and 20 older (68-85 years) adults. Finally, using minute-by-minute HR and mean arterial blood pressure (MAP) time series from a cohort of over 450 ICU patients in the MIMIC II database [23], we evaluated the performance of our approach in capturing the HR/BP coupling differences between patients with vs. without severe sepsis.

II. Materials and Methods

A. Model

Figure 1 presents a schematic diagram of the proposed algorithm for model-based analysis of multivariate time series in a nonstationary setting. As depicted in Panel (a), we employed SVAR processes to model a physiological time series cohort via Markov transitions among a collection of simpler linear dynamical systems [21]. For the n-th patient ($n = 1 \cdots N$), let $y_t^{(n)}$ be a $M \times 1$ vector of observed values of the vital signs at time t ($t = 1 \cdots T^{(n)}$). We assume that there exists a library of J possible dynamics or *modes*; parameterized by $\theta_j = \{\mathcal{A}^{(j)}, Q^{(j)}\}_{j=1}^{J}$, where $\mathcal{A}^{(j)} = \{a_p^{(j)}\}_{p=1}^{P}$ is a set of multivariate autoregressive model coefficient matrices of size $M \times M$, with maximal time lag P, and the corresponding noise covariance $Q^{(j)}$.

Let $s_t^{(n)}$ be a switching variable indicating the active dynamic mode of the n-th patient at time t, and evolving according to a Markovian dynamic with initial distribution $\pi^{(n)}$ and a $J \times J$ transition matrix Z. Following these definitions, an SVAR model for the n-th patient is defined as:

$$y_t^{(n)} = \sum_{p=1}^{P} a_p^{(s_t^{(n)})} y_{t-p}^{(n)} + w^{(s_t^{(n)})} \ , w^{(s_t^{(n)})} \sim \mathcal{N}(0, Q^{(s_t^{(n)})}) \ . \tag{1}$$

where the fluctuation term $w^{(s_t^{(n)})}$ is assumed Gaussian distributed with covariance $Q^{(s_t^{(n)})}$.

A collection of nonstationary multivariate time series can be modeled as switching among these J dynamic behaviors, each describing a locally coherent linear model that persists over a segment of time. Inference was performed as in [21] to learn the set of switching variables (i.e., segmentation of the time series) and the modes (i.e., the parameters θ). Briefly, we used expectation-maximization (EM) [21] to find the maximum-likelihood set of model parameters (M step), as well as a factored estimate of the posterior distribution over the latent switching variables (E step). Sharing of the dynamics across the entire cohort was achieved by pooling together all calculated and inferred statistics across all the subjects (from the E step) to learn a *shared* set of modes in the M step. Iteration through several steps of the EM algorithm resulted in learning a set of j shared modes and a global transition matrix Z for all the patients. We define the term *mode proportion*, $\eta_j^{(n)}$, to denote the proportion of time the n-th patient spends within the j-th mode. Given the learned distribution of the switching variables s_t from the EM algorithm, we have

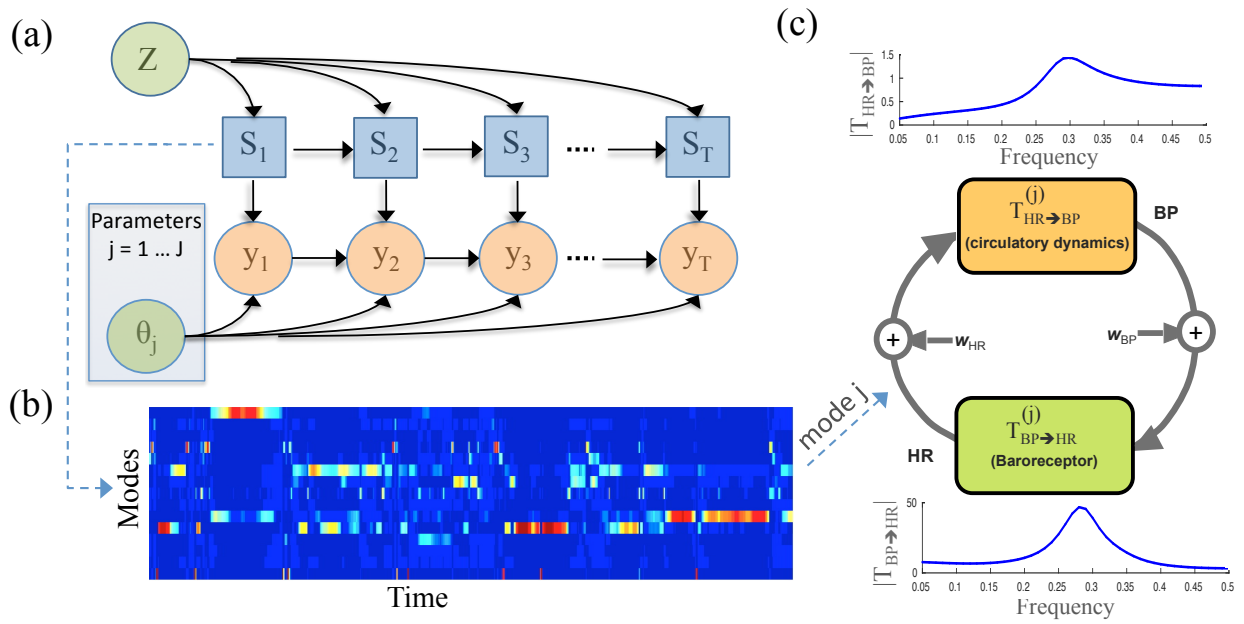

Fig. 1. Schematic diagram of the proposed algorithm. The graphical model representation of a switching vector autoregressive (VAR) model is shown in panel (a). A given dynamical mode is defined in terms of a set of VAR coefficients and the corresponding noise terms (θ_j; see main text), and switching among the different modes is governed by a Markov chain with transition matrix Z. An illustrative example of marginal probabilities of the switching variables is shown in panel (b), with colors blue and red denoting the low and high probability modes, respectively. Each VAR model corresponds to a set of coefficients that can be used to describe the interaction among the observed variables both in time and frequency domain. For instance, assuming input variables are heart rate (HR) and blood pressure (BP) ($y = [HR\ BP]^T$), the VAR parameters can be used to derive the frequency-dependent transfer functions corresponding to the Baroreflex control of HR in response to changes in BP, and the "circulatory dynamics" effects [24] which capture the influence of changes in HR on BP, as depicted in panel (c) and described in section II-A.

$$\eta_j^{(n)} = \frac{1}{T^{(n)}} \sum_{t=1}^{T^{(n)}} Pr(s_t^{(n)} = j) \tag{2}$$

where Pr denotes the probability, and the entire quantity inside the summation is the inferred state marginal probabilities, which are calculated during the E step.

1) Calculations of Gain and Power Spectrum: For the j-th mode, the AR coefficients $\mathcal{A}^{(j)}$ can be used to drive the transfer functions between any two variables, and to extract the parametric power spectra of each variable. The transfer function analysis enables us to quantify the frequency dependent influence of any one variable on any of the remaining $M-1$ variables. For instance, in the bivariate case ($M = 2$), with HR and BP as the variables of interest, the transfer function between BP and HR (denoted as $T_{BP\rightarrow HR}$) describes the influence of changes in BP on HR at different frequencies (see Fig. 1, panel (c)).

Mode-Specific Transfer Function Gains and Power Spectra: Given a dynamic mode j and any two variables l and m, the block transfer function of the two variables can be defined as a function of the AR parameters. Let

$$A_{l,m}^{(j)}(f) = \sum_{p=1}^{P} a_p^{(j)}[l,m] \cdot e^{-2\pi\sqrt{-1}fp}, \tag{3}$$

where f is the index of frequency. The relationship between the variables l and all other variables in the frequency domain can be represented as the following [20]:

$$y_l(f) = \frac{1}{1 - A_{l,l}^{(j)}(f)} [\sum_{k \neq l} A_{l,k}^{(j)}(f) y_k(f) + w_l(f)]. \tag{4}$$

For instance, in the bivariate case, with variables l and m we have:

$$y_l(f) = \frac{A_{l,m}^{(j)}(f)}{1 - A_{l,l}^{(j)}(f)} y_m(f) + \frac{1}{1 - A_{l,l}^{(j)}} w_l(f) \tag{5}$$

$$y_m(f) = \frac{A_{m,l}^{(j)}(f)}{1 - A_{m,m}^{(j)}(f)} y_l(f) + \frac{1}{1 - A_{m,m}^{(j)}} w_m(f) \tag{6}$$

Assuming l and m represent HR and BP respectively, the transfer function $T_{m\rightarrow l}^{(j)} = \frac{A_{l,m}^{(j)}(f)}{1 - A_{l,l}^{(j)}(f)}$ captures the effect of BP variability on heart rate, and the *Baroreflex gain* can be estimated as the absolute value of this transfer function. On the other hand, the transfer function $T_{l\rightarrow m}^{(j)} = \frac{A_{m,l}^{(j)}(f)}{1 - A_{m,m}^{(j)}(f)}$ captures the mechanical effect of HR variability on BP [25], [8], [24] via the Windkessel function [8] or the circulatory dynamics [24].

In the analysis involving HR and RESP, the *RSA* gain, which measures the respiratory modulation of heart rate, can be derived similarly. Furthermore, we derive the parametric power spectra corresponding to the individual modes using the autoregressive coefficients:

$$P^{(j)}(f) = H^{(j)}(f) Q^{(j)} H^{(j)}(f)^{\top}, \tag{7}$$

where $H^{(j)}(f) = (I - A^{(j)}(f))^{-1}$, and $P^{(j)}_{l,l}(f)$ and $P^{(j)}_{m,m}(f)$ define the power spectra of the l-th and m-th variables, respectively.

Nonstationary Power Spectral and Transfer Function Analysis: Given the inferred state marginal probabilities from the SVAR model, one can compute the patient-specific "mode-proportioned" transfer function gains and power spectra as:

$$T^{(n)}_{l\to m}(f) = \sum_{j=1}^{J} \eta^{(n)}_j |T^{(j)}_{l\to m}(f)|, \tag{8}$$

$$P^{(n)}_{l,m}(f) = \sum_{j=1}^{J} \eta^{(n)}_j |P^{(j)}_{l,m}(f)| \ . \tag{9}$$

Similarly, the *instantaneous* transfer function gains and power spectra can be computed via a weighted combination of the associated quantities for the individual modes, where the weights are given by the state marginal probabilities $Pr(s^{(n)}_t = j)$.

B. Dataset

1) Tilt-Table dataset: The tilt-table dataset, publicly available via PhysioNet [26], contains HR and BP recordings from 10 healthy subjects (five males, five females) undergoing a tilt-table test of orthostatic tolerance [27]. The mean age was 28.7 $\pm$ 1.2 years. The details of the protocol are described in Heldt et al. [27]. Briefly, subjects were placed in a supine position. Tilting was performed from horizontal position to vertical position and back to supine. All waveforms were recorded at 250 Hz sampling frequency, for approximately 60 minutes (varying from 55 to 74 minutes) per subject. Each heartbeat was annotated using an automated beat detection algorithm, and the blood pressure time series was sampled for each RR interval at the times of the R wave peaks. Since we were interested in the dynamics of interaction between HR and BP in the frequency range pertinent to sympathetic and parasympathetic regulation [1], time series of HR and BP were high-pass filtered to remove the steady-state baseline and any oscillation in the time series slower than 100 beats/cycle. This filtering was done using a 7th order Butterworth digital filter with cutoff frequency of 0.01 cycles/beat.

2) Fantasia: Time series of heart rate and respiration were extracted from the Fantasia database publicly available at the PhysioNet [6], [26], consisting of 20 young subjects (21 to 34 years) and 20 older adults (68 to 85 years). Each group had equal numbers of males and females (10 in each group). The subjects underwent 120 minutes of continuous monitoring in resting supine position while watching the movie Fantasia. Continuous time-synchronized measurements of electrocardiogram (ECG) and respiration (impedance plethysmography) were collected in all subjects. All waveforms were recorded at 250 Hz sampling frequency.

We used the automatically detected, visually verified and corrected ECG R-peak annotations available on the PhysioNet website [26] to derive time series of peak-to-peak (RR) intervals. To derive the corresponding respiratory time series, we first removed the baseline drift (often seen in impedance plethysmography-based measurement of respiratory volume) by fitting a cubic spline function through all the breath onsets, and subtracting the resulting baseline curve from the respiratory waveform; the resulting volume waveform started at zero upon the onset of each breath. Next, we constructed a respiratory volume time series for each RR interval from the volume difference at the times of the R wave peaks, as previously described in Nemati et al. [28].

3) MIMIC II: The MIMIC II database [23], publicly available via PhysioNet [26], includes clinical (laboratory values, IV medications, etc.) and physiological data (heart rate, blood pressure, oxygen saturation, etc.) collected from the bedside monitors (Component Monitoring System Intellivue MP-70; Philips Healthcare, Andover, MA) in ICUs of the Beth Israel Deaconess Medical Center (BIDMC) in Boston. This study included 453 adult patients from the MIMIC II waveform database [23] with clinical information, and at least eight hours of continuous minute-by-minute HR and invasive BP measurements during the first 24 hours of their ICU stays. The data set contained over 9,000 hours of minute-by-minute HR and invasive mean arterial BP measurements (over 20 hours per patient on average) from 453 adult patients. HR and BP time series were detrended by removing the mean. Gaussian noise was used to fill in for the missing blocks (median length of 3 minutes with interquartile range of [2,9] minutes) of data. (This allows for all missing data blocks to get assigned to a single dynamic mode.)

Among the 453 patients, 106 were determined to have had severe sepsis during the first 24 hours of their ICU stay, using the criteria described next. Approximately 30% of the patients (139 out of 453) had severe sepsis at some point during their hospital stays based on the Angus criteria; as indicated by their International Classification of Diseases (ICD-9) codes [29]. Patients who met the Angus sepsis criteria were screened to establish their status of having sepsis on first day of ICU admission based on the SIRS criteria, microbiology culture test (with cultures sampled for microbiology test within 48-hours from the start of ICU admission or 24-hours post ICU admission), antibiotics prescription (prescribed within 48-hours from the start of ICU admission or 24-hours post ICU admission), and mentioning of sepsis or infections in the nursing notes during the first 24-hours in the ICU. The status of severe sepsis on first day of ICU admission was identified as sepsis (as described above) with tissue hypoperfusion or organ dysfunction indicated by any of the following: hypotension (MAP decrease to 60mmHg or lower), acute kidney injury (creatinine at least 50% or $>$ 0.3 mg/dL increase from baseline), acute lung injury as indicated by the use of mechanical ventilation, lactate above 2 mmol/L, bilirubin $>$ 2mg/dL, plateletes $<$ 100,000uL, coagulopathy (International Normalized Ratio or INR $>$ 1.5) [30].

C. Model Parameter Setting

We modeled the beat-by-beat HR/BP time series for the tilt dataset and the HR/Resp time series for the Fantasia dataset as a switching AR(5) process to model most of the parasympathetic responses and at least some of the sympathetic effects, without introducing an unduly complex model. Minute-by-minute HR and BP time series from MIMIC II

were modeled as a switching AR(5) process to capture two real oscillations and a possible trend per mode; the number of dynamic modes (J=25) was determined with the Bayesian Information Criterion (BIC) [31] using the bi-variate HR/MAP data. Similarly, based on the BIC criteria, four dynamic modes were used for both the Tilt-table and the Fantasia datasets.

D. Analysis and Evaluation

Transfer function gains and spectral power were calculated and reported as a function of frequency; specifically, periods of 2 to 20 beats (or 0.5 to 0.05 cycles-per-beat) for the Tilt and Fantasia, and periods of 3 minutes to 4 hours (0.3242 - 0.0042 cycles-per-minute) for the MIMIC II dataset. For beat-to-beat analysis, frequency was defined by cardiac beats (or cycles/beat). For beat-to-beat HR, LF/HF ratio was computed as the ratio of the low (LF: periods of 7-20 beats) to high (HF: periods of 2-6 beats) frequency power of the HR. In addition to reporting frequency-specific gains, patient-specific mean gains were computed by averaging mode-proportioned gains, over the entire frequency range unless otherwise specified.

Non-parametric Wilcoxon rank-sum test was used to assess the differences in the derived spectral and coupling indices (i.e., spectral powers, LF/HF HR power ratios, and gains) between different outcome groups (i.e., supine vs. non-supine, young vs. old, or absence vs. presence of severe sepsis). Additionally, we used logistic regressions to examine the associations between mode proportions (or mode-specific gains) and outcomes. Two-sided P values less than 0.05 were considered statistically significant. In tests that involve frequency-by-frequency or mode-specific multiple comparisons, test of statistical significance was based on P values after correcting for multiple comparisons using FDR (false discovery rate) [32].

In the MIMIC II study, multivariable logistic regression association analysis was conducted on the top ten most common dynamic modes to test the association between dynamic modes and severe sepsis. In the multivariable logistic regression analysis, we report the adjusted P values and odds ratios (ORs) with 95% confidence intervals (CI). The dynamic mode proportion or gain were the primary predictive variables; APACHE-III [33] and interventions (use of sedatives, pressors, mechanical ventilation, and pacemaker) were added as confounding co-variates. The Hosmer-Lemeshow (HL) P values were reported to assess the model fit, with values of over 0.05 indicating a good fit. Dynamic modes were considered as high-risk or low-risk based on their odds ratios from logistic regression analysis with severe sepsis as an outcome measure.

In evaluating the classification performance of our approach in detecting severe sepsis, we characterized each time series with its corresponding mode proportioned gains (a $1 \times K$ feature-vector, where K is the number of frequencies) as features, and used a logistic regression classifier with 10-fold cross validation. Comparison of area under the receiver operating curves (AUCs) was based on the method described in [34].

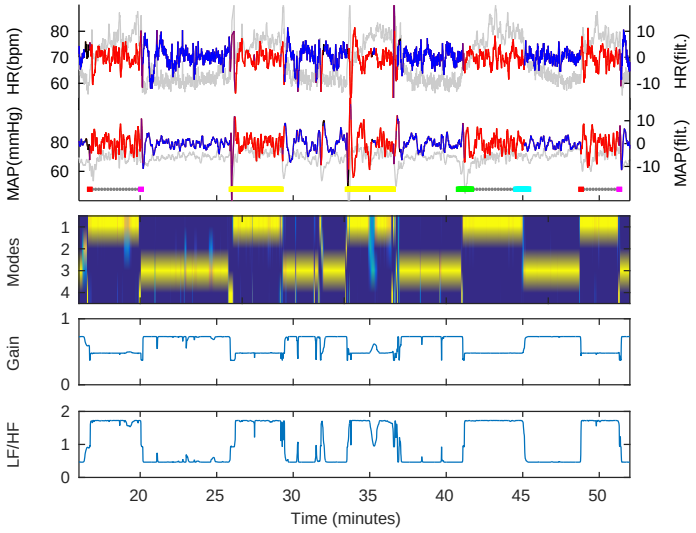

Fig. 2. Example segmentation (top panel) and the derived instantaneous gain and LF/HF ratio of the HR/BP recordings a subject from the Tilt table study. In the top panel, the color indicates the inferred dynamic mode assignment. The algorithm consistently assigned the Mode 1 (red) to the non-supine position. The supine position was captured by Mode 3 (blue). The second panel shows the state marginal probability of the observations belonging to each mode, with the yellow color denoting high probability mode. The third and fourth panels plot the calculated gain and HR power LF/HF ratio respectively for the same subject, as the subject transitions between dynamic Mode 3 (blue) and Mode 1 (red) while alternating between supine and non-supine positions. The third and fourth panel show the instantaneous mean baroreflex gain and the LF/HF HR power ratios over time respectively, calculated from learned AR coefficients weighted by mode proportion at each beat. For the top panel, actual values were in gray (Y-axis on left) and filtered values (Y-axis on right) were color-coded based on the inferred dynamical modes. Annotations for the actual tilt procedures performed were plotted as horizontal bars on the bottom of the top panel and are color coded (green to cyan: slow tilt up and down to supine; red to pink: rapid tilt up and down to supine; yellow: stand up and back to supine).

III. Results

A. Tilt

We evaluated the performance of our approach in capturing the autonomic changes corresponding to tilting procedures by comparing the baroreflex gains and the LF/HF HR power ratios (an index of sympathetic activation) between the supine vs. the non-supine segments. Figure 2 shows the SVAR segmentation of the HR and MAP time series of one of the 10 subjects, while alternating between supine and non-supine positions. The third and fourth panel of Fig. 2 show the instantaneous mean baroreflex gains and the LF/HF HR power ratios of Subject 1 over time, respectively. The gains were calculated from the learned AR coefficients weighted by the state marginal probabilities on a beat-by-beat basis. Note that SVAR is able to track changes in baroreflex gains and HR power LF/HF ratios as the subject alternates between supine vs. non-supine positions.

Next, we compared the LF/HF HR power ratios and the baroreflex gain of the supine vs. the non-supine positions calculated using all 130 time series segments (70 supine and 60 non-supine segments) from ten subjects. For each of the 130 time series segments, we calculated the mode-proportioned gains; the LF/HF ratios were computed similarly, with the LF range corresponding to periods of 7-20 beats, and HF range

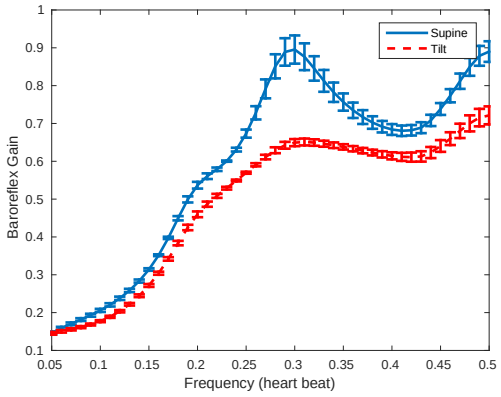

(a) Tilt: Baroreflex Gain Supine vs. Non-Supine

Fig. 3. Tilt: comparison of computed baroreflex gains in supine vs. non-supine positions. Plot shows means and standard errors.

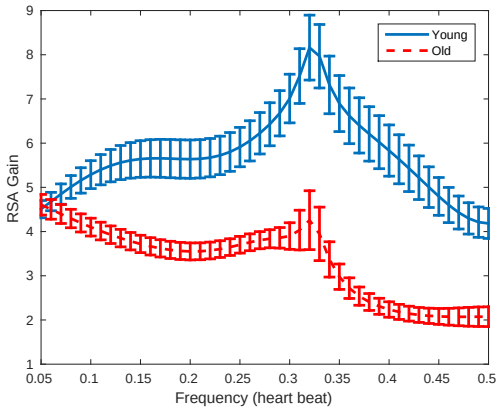

(a) Fantasia: RSA gains young vs. old

Fig. 4. Fantasia: RSA gains of the young vs. the old. Plot shows means and standard errors. Old and young subjects were statistically significantly different in their RSA gains when frequencies were $\geq$ 0.15 (P$\leq$0.001), and in particular in the frequency range $\geq$ 0.29 (P$\leq$0.0001).

corresponding to periods of 2-6 beats.

Table I shows the population medians and interquartiles (IQRs) of the LF/HF ratios and the mean baroreflex gains of the supine (70 time series segments) vs. the non-supine positions (60 time series segments). The P values shown were from the Wilcoxon test. We observed an increase in the ratio of the low (LF: periods of 7-20 beats) to high (HF: periods of 2-6 beats) frequency power of the HR (also known as the LF/HF ratio) from supine to tilting. Table I confirms that the LF/HF ratios of the non-supine (tilt) positions were larger than those in the supine positions, and that the baroreflex gains of the non-supine (tilt) positions were smaller than those in the supine positions. These results are consistent with prior studies involving posture induced changes in autonomic function that reported a significant increase in LF/HF ratios and a reduction in baroreflex gains in the upright positions due to an enhanced sympathetic drive [5], [25].

	Supine	Non-Supine	P
LF/HF	0.91 [0.62, 1.07]	1.44 [1.33, 1.55]	$<$ 0.0001
Baroreflex Gain	0.57 [0.54, 0.65]	0.49 [0.47, 0.52]	$<$ 0.0001

TABLE I
TILT: LF/HF RATIOS AND MEAN GAINS DURING SUPINE VS. NON-SUPINE POSITIONS. POPULATION MEDIANS [INTERQUARTILES] SHOWN.

Figure 3 shows a comparison of the baroreflex gains of the supine vs. the non-supine positions across the power spectra (between 0.05 to 0.5 cycles-per-beat). Non-parametric Wilcoxon ranksum tests on frequency-by-frequency comparison of the gains (in the frequency range $\geq$ 0.1) between the two groups with FDR adjustment for multiple comparisons confirmed that the baroreflex gains of the supine positions were statistically significantly smaller than those of the non-supine (tilt) positions, particularly in the frequency range between 0.1 to 0.3 cycles-per-beat (P$\leq$0.0001).

B. Fantasia

Using the Fantasia dataset, we evaluated the performance of our approach in capturing the differences between the old vs. the young subjects in terms of their autonomic functions by comparing their mode-proportioned RSA gains and the LF/HF HR power ratios. Our results indicated that the young and the elderly subjects exhibit distinctly different mode distributions. Association analysis showed that both Modes 1 and 2 were significantly associated with aging; Mode 1 had a significantly higher odds for aging (P=0.0084, OR=1.47 [1.10 1.96]), while Mode 2 had a lower odds for aging (P=0.0162, OR=0.57 [0.37 0.90]). Using 10-fold cross validation, the classification performance (young vs. old) using the mode proportions from all four modes achieved a median [interquartiles] AUC of 1.00 [0.75, 1.00]. Mode 1 had a mode-specific RSA mean gain of 3.31, and LF/HF HR power ratio of 0.48. Mode 2 had a higher mode-specific mean gain of 8.65, and LF/HF HR power ratio of 0.13. These results indicate that the dynamic mode with a significantly higher odds of aging had a blunted RSA.

	Young	Old	P
LF/HF	0.40 [0.22, 0.50]	0.51 [0.48, 0.55]	0.0016
RSA Gain	5.54 [4.01, 7.65]	3.20 [2.94, 3.71]	0.0001

TABLE II
FANTASIA: LF/HF RATIOS AND MEAN GAINS FOR YOUNG VS. OLD. N=40.

Table II shows the population median and interquartile range of mode-proportioned LF/HF HR power ratios and the mode-proportioned mean RSA gains of the old vs. the young subjects. We observed a decrease in the RSA gains and an increase in the ratio of the low (LF: periods of 7-20 beats) to high (HF: periods of 2-6 beats) frequency power of the HR in the old. The increase in the LF/HF HR power ratios among the old is consistent with prior findings which reported a reduction in high-frequency contribution of respiration to heart rate variability patterns due to aging [28].

Figure 4 shows a comparison of the RSA gains of the young vs. the old across the power spectra. Non-parametric Wilcoxon ranksum tests on frequency-by-frequency comparison of RSA gains (in the frequency range $\geq$ 0.1) between the two groups with FDR adjustment for multiple comparisons confirmed that the RSA gains of the old were statistically significantly smaller than those of the young in the frequency range $\geq$ 0.15

	ALL	No Severe Sepsis (N=347)	Severe Sepsis (N=106)	P
Male(%)	59%	63%	45%	0.001
Age	69 [57, 79]	68 [57, 77]	71 [58, 80]	0.12
Hosp. Mort.	15%	9%	34%	<0.0001
ICU LOS	4.00 [2.27, 7.67]	3.38 [2.02, 5.84]	7.91 [3.68, 15.82]	<0.0001
Hosp. LOS	9.00 [6.00, 15.00]	8.00 [6.00, 12.00]	14.00 [8.00, 24.00]	<0.0001
ICU (CCU/CSRU/MICU/SICU)	21% / 42% / 26% / 12%	20% / 55% / 13% / 12%	23% / 1% / 67% / 9%	-
Pressor/MV/Sedative	57% / 32% / 65%	59% / 20% / 67%	53% / 72% / 57%	-
Primary Diagnosis	Coron Atheroscler Native (19%)	Coron Atheroscler Native(24%)	Septicemia Nos(10%)	-
	AMI, Subendocard Infact(8%)	AMI, Subendocard Infact(10%)	Respiratory Failure(8%)	-
	Aortic Valve Disorder(6%)	Aortic Valve Disorder(7%)	Pneumonia, Organism Nos(7%)	-
Co-morbidities	Hypertension(76%)	Hypertension(68%)	Congestive Heart Failure(35%)	-
	Congestive Heart Failure(73%)	Diabetes(57%)	Chronic Pulmonary(20%)	-
	Diabetes(70%)	Chronic Pulmonary(48%)	Cardiac Arrhythmias(17%)	-

TABLE III
MIMIC II PATIENT CHARACTERISTICS: COMPARISON OF PATIENTS WITH AND WITHOUT SEVERE SEPSIS. LOS - LENGTH-OF-STAY (DAYS). MV - MECHANICAL VENTILATION. AMI - ACUTE MYOCARDIA INFARCTION. CCU - CORONARY CARE UNIT. CSRU - CARDIAC SURGERY RECOVERY UNIT. MICU - MEDICAL INTENSIVE CARE UNIT. SICU -SURGICAL INTENSIVE CARE UNIT.

cycles-per-beat (P$\leq$0.001) and, in particular in the frequency range $\geq$ 0.29 (P$\leq$0.0001). These results are consistent with previously established findings [28] that aging is associated with a diminished autonomic control.

C. MIMIC II

Table III displays the patient characteristics, including the most prevalent primary diagnosis as well as co-morbidities (based on the ICD-9 codes) from the MIMIC II cohort; P values are from Wilcoxon ranksum test for continuous variables, and from chi-square test for proportions. As expected, patients with severe sepsis tended to have longer ICU and hospital length-of-stays, and had higher hospital mortality. We also note that patients with severe sepsis had different distributions in primary diagnosis, co-morbidities, and care units than the ones without.

We performed multivariable logistic regression analysis to identify dynamic modes which were significantly associated with severe sepsis (see Table VI in Appendix A). Mode proportion of individual mode for each patient was used as a primary predictive features. Our results indicate that three dynamic modes (2, 5, and 9) were significantly associated with severe sepsis even after adjustment for interventions and APACHE-III: mode 2 was associated with an increased odds of sepsis (adjusted P=0.0001, OR with 95% CI 1.64 [1.28, 2.11]) and therefore was considered "high-risk mode'. Modes 5 and 9 were associated with a lower odds of severe sepsis (mode 9 - adjusted P=0.0022, OR with 95% CI 0.23 [0.09, 0.59], mode 5 - adjusted P=0.0095, OR with 95% CI 0.34 [0.15, 0.77]) and were thus considered "low-risk modes".

Figure 5 plots the bivariate dynamic modes 2, 5 and 9 and the frequency-specific gains of the three modes. Note that the high-risk mode 2 appeared to have low gains across all frequency spectra; whereas the low-risk modes 5 and 9, on the contrary, had a distinct peak in HR/MAP gains at the LF range of 0.16-0.18 cycles-per-minute (0.0027 - 0.003 Hz) or 5-6 minutes cycle.

Figure 6 shows an example learned HR/MAP segmentation from SVAR, of two patients with and without severe sepsis, over a five-hour period during the first day in the ICU. The corresponding dynamic state marginals, and gains of each patient are also shown. Note that the patient with severe sepsis (panel b) spent significant proportion of time in the high-risk mode 2 (red); whereas the patient without severe sepsis (panel a) exhibited high mode proportions in low-risk dynamic modes 5 (purple) and 9 (green), and had higher gains in comparison to the patient with severe sepsis.

1) Frequency-by-Frequency Comparison of HR/MAP Gain and Spectral Power between Patients with and without Severe Sepsis: Figure 7 compares patients with and without severe sepsis using mode-proportioned HR/MAP gains and spectral power. Only modes with significant association with severe sepsis after adjusting for APACHE-III and interventions (modes 2, 9 and 5) were included to compute the mode-proportioned gains or spectral power. For HR/MAP gains (Figure 7a), the most statistically significant association occurred at the frequency range of 0.1342 - 0.1942 cycles-per-minute (approximately 5 to 7 minute cycle) after adjusting for interventions (P=0.0001). With FDR adjustment, the gains remained statistically significantly associated with severe sepsis (P<0.01 for over 85% of the frequencies examined). Non-parametric ranksum tests on frequency-by-frequency comparison of mode-proportioned HR/MAP gains (in the frequency range between 0.1 and 0.3) between the two groups with FDR adjustment for multiple comparisons confirmed that the gains of the severe sepsis group were statistically significantly smaller than those without (P$\leq$0.0002).

2) Severe Sepsis Classification Performance: Table IV shows the 10-fold cross-validated classification performance of our approach using the mode-proportioned gains or powers in the frequency range [0.1, 0.3] cycles-per-minute to identify patients with severe sepsis. HR/MAP gains achieved an AUC of 0.74 [0.68, 0.79]). State-of-the-art APACHE-III achieved a higher AUC of 0.79 [0.74, 0.85]), though the differences were not statistically significant (P=0.10). Combining the bivariate gains and APACHE-III yielded a slight improvement in APACHE-III's performance from an AUC of 0.79 [0.74,0.85] to 0.82 [0.77, 0.87] (P=0.12). Combining the HR or MAP power and APACHE III achieved similar performance.

3) Comparison of Mean HR/MAP Gains and Spectral Power between Patients with and without Severe Sepsis: Table

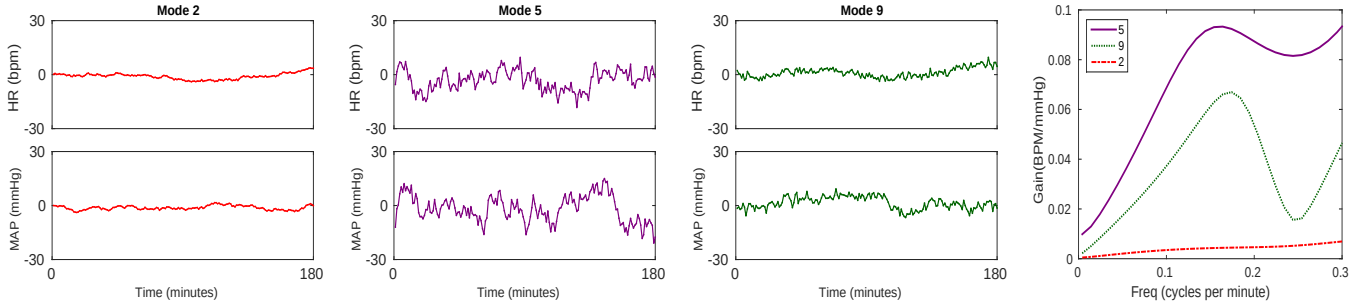

(a) **Mode 2 (high-risk)** (b) **Mode 5 (low-risk)** (c) **Mode 9 (low-risk)** (d) Gain

Fig. 5. Example HR and MAP bivariate dynamic modes significantly associated with severe sepsis in the ICU, even after adjusting for interventions and severity of illness scores. All three modes were simulated from their AR coefficients and covariances; their frequency-specific gains are shown in panel (d).

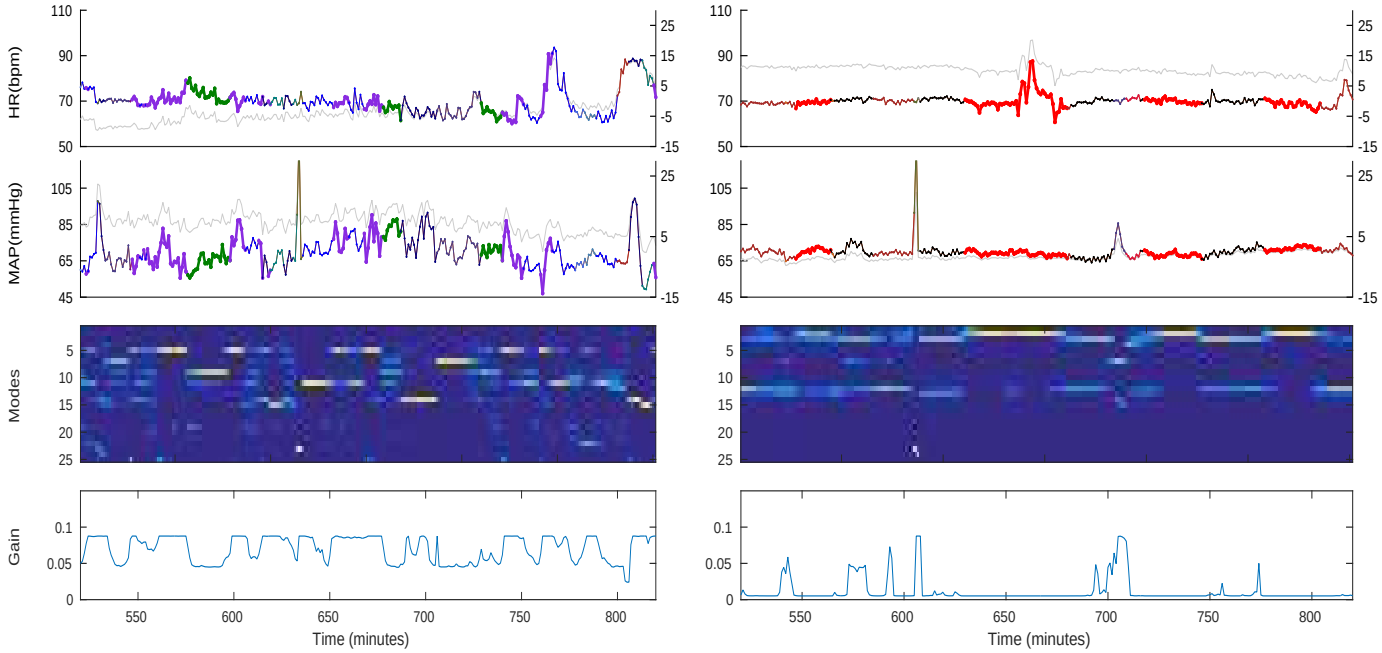

(a) Patient without severe sepsis (b) Severe sepsis patient

Fig. 6. Learned SVAR segmentation of heart rate and mean arterial BP of two patients with and without severe sepsis. Plot shows five hours of recordings during the first 24 hours patients were in the ICU. HR and mean arterial BP measurements plotted in original units in gray; detrended measurements in color. Samples were color coded by their mode assignment. Both patients were from the same test set, with dynamic modes learned from the corresponding training set. Mean gains were weighted by mode proportions of modes 2 (Red), 5 (Purple) and 9 (Green). The next panel shows the state marginal probability of the observations belonging to each mode, with the yellow color denoting high probability mode. The bottom panel shows the instantaneous mean gain over time.

	AUC (95% CI)	Sens.	Spec.
HR,MAP$_{gain}$	0.74 [0.68, 0.79]	0.74	0.60
HR$_{power}$	0.73 [0.67, 0.79]	0.69	0.65
MAP$_{power}$	0.72 [0.66, 0.78]	0.68	0.63
APACHE-III	0.79 [0.74, 0.85]	0.81	0.71
HR,MAP$_{gain}$+APACHE-III	0.82 [0.77, 0.87]	0.74	0.78

TABLE IV
PERFORMANCE OF SEVERE SEPSIS CLASSIFICATION. AUC, SENSITIVITY, AND SPECIFICITY SHOWN.

	Non-Sev. Sepsis	Sev. Sepsis	P	P$_{adj}$
Gain	0.05[0.03,0.06]	0.03[0.01,0.06]	0.0001	0.0003
HR$_{power}$	15.76[7.50,19.95]	7.45[1.52,16.93]	0.0001	0.0002
MAP$_{power}$	13.35[6.16,16.15]	6.15[1.29,14.52]	0.0001	0.0001

TABLE V
COMPARISON OF HR/MAP MEAN GAINS AND POWER SPECTRAL CONTENT OF PATIENTS WITH SEVERE SEPSIS (N=106) VERSUS THOSE WITHOUT (N=347). P$_{adj}$ INDICATES ADJUSTED P VALUE.

V compares the HR/MAP mode-proportioned *mean* gains and power spectra of patients with and without severe sepsis. Mean gains and spectral powers were computed by averaging over the frequency range of (0.1, 0.3) cycles per minute. Our results indicate that HR/MAP mean gains and power spectra were significantly associated with severe sepsis (P$\leq$0.001) even after adjusting for interventions. Ranksum test confirmed that patients with severe sepsis had statistically significantly lower mean gains and HR/MAP power spectral content than those without (P$<$0.0001).

IV. DISCUSSION AND CONCLUSIONS

We presented a switching linear dynamical systems based framework for learning physiologically interpretable features

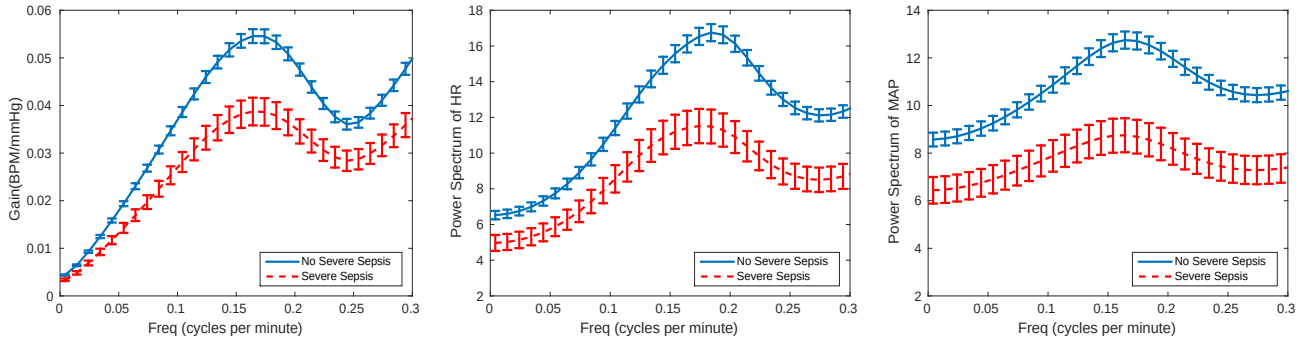

(a) HR/MAP gains (b) HR spectral power (c) MAP spectral power

Fig. 7. MIMIC II: comparison of patients with and without severe sepsis in (a) frequency-specific HR/MAP gains, (b) HR spectral power, and (c) MAP power spectral content. Plot shows means and standard errors. For HR/MAP gains (a), the most statistically significant association occurred at the frequency range of 0.1342 - 0.1942 cycles-per-minute (approximately 5 to 7 minute cycle) after adjusting for interventions (P=0.0001). For HR power (b), the most statistically significant association occurred at the frequency range of 0.1842 - 0.2742 cycles-per-minute (approximately 3 to 5 minute cycle) after adjusting for interventions ($P<=0.0001$). For MAP power (c), the most statistically significant association occurred at the frequency range of 0.1542 - 0.2342 cycles-per-minute (approximately 4 to 6 minute cycle) after adjusting for interventions ($P\leq 0.0001$).

in time series of vital signs from a patient cohort. The method is fully multivariate, handles nonstationarity, and can be used to extract spectral signatures of the individual vital-sign time series, as well as transfer functions pertinent to autonomic regulation. The proposed approach incorporates models of autonomic controls within a machine learning framework to provide mechanistic interpretation of the learned dynamics, allowing one to identify possible physiological mechanisms (e.g., baroreflex) driving the cardiovascular oscillations, and study how directional influences and spectral power at specific frequency bands are altered in aging or diseased states.

The tilt-table and the Fantasia datasets were used to validate the ability of our approach in modeling baroreflex and RSA gains, which have been widely studied as indices of autonomic regulation [35], [25], [36], [37]. We showed that the proposed technique can reliably detect alterations in cardiovascular and cardiopulmonary control parameters due to orthostatic stress and aging. In the tilt table study, we demonstrated that our approach was able to automatically identify dynamic modes corresponding to sympathovagal activation due to a postural change from supine to non-supine position. We observed an increase in the LF/HF HR power ratios and a decrease in the baroreflex gain when subjects were transitioned to a non-supine position, indicating possible sympathetic activation. In the Fantasia study, our analysis showed a significant reduction in the RSA gain in the elderly population, consistent with previous results that aging is associated with a blunted autonomic control [38].

We investigated the low-frequency spectral characteristics and coupling strengths of non-stationary HR and BP time series for patients in ICUs and their associations with severe sepsis using minute-by-minute heart rate and blood pressure time series from the MIMIC II database. Our findings indicate that reduced HR/MAP coupling is significantly associated with severe sepsis even after adjusting for clinical interventions ($P\leq 0.001$). The diminished HR/MAP variability and gains of the severe sepsis patients may reveal a breakdown of the inter-organ communication and coupling due to inflammatory responses [39], [40], which are known to have downstream effects on the sympathetic and parasympathetic components of the heart rate and blood pressure variability [41]. These findings are in accordance with the "uncoupling" hypothesis [42], [43] that sepsis and progression into severe sepsis and multiple organ dysfunction syndrome reflects progressive uncoupling among physiological regulatory mechanisms.

By jointly modeling multivariate time series from a cohort of patients, our approach enabled discovery of phenotypic dynamic modes that correspond to nonstationary changes within a subject and phenotypic differences across subjects. We demonstrated that such a framework can be used to quantify the association between a given clinical condition and vital-sign dynamics at a population level. In the MIMIC II study, we observed that patients with the severe sepsis exhibited dynamic behaviors with significantly reduced low-frequency oscillations and gains than those without; the association remained significant even after adjusting for interventions. Studies that examined low-frequency oscillations and gains of multivariate vital-sign time series and their associations with pathophysiological conditions in a critical care setting have been sparse. Our findings suggest that patients who exhibited dynamic modes with a distinct peak at the 5-7 minute cycle in the HR/MAP gains had a significantly lower odds of having severe sepsis. Low frequency modulations of HRV (between 0.025 and 0.07 Hz) have been attributed to influences from renin-angiotensin system, endothelial factors, local influences related to thermoregulation, and others [11]. The source of the very low-frequency modulation and coupling at 3-7 minutes cycle that characterized "healthier" patients in our MIMIC II cohort remains to be elucidated, but is likely due to thermoregulatory vasomotor control [44].

Several prior works have investigated the prognostic values of HR and BP variability for early detection of neonatal sepsis and prediction of clinical outcomes [45], [46], [47], including variants of the switching linear dynamical systems model presented here [48], [49], [19], [50]. However, previous approaches have been primarily focused on outcome prediction or classification of the physiological states, rather than providing mechanistic interpretations of the observed

dynamics. While previous works on cross-spectral techniques also assessed coupling among physiological variables [13], [14], our approach addresses the problem of nonstationarity of physiological time series in realistic settings. The time-varying vector autoregressive (VAR) models have been used [51], [18] to quantify the cardiovascular and respiratory feedback loops. Our approach differs from these previous works in that we explicitly account for dynamic regime changes, and jointly model multivariate dynamics of time series to learn the shared dynamics across a heterogeneous patient cohort. Finally, the prognostic value of each dynamic mode can be determined using a logistic regression classifier and therefore enable analysis to focus on the most predictive modes for a given clinical question.

In an ICU environment, changes in dynamics reflect the underlying pathological processes as well as interventions aimed at restoring normal physiological states. However, these states are often defined in terms of mean values of the vital signs, and the notion of normality is defined with respect to the healthy individuals and at the population level. There remains significant controversy regarding the normal range of vital signs in the critically ill patients under various pathological conditions [52], [53]. Given the importance of healthy variability and autoregulatory mechanisms, it has been suggested that goal-directed therapies should aim at restoring the healthy vital signs variability and coupling [54], [55]. Future work may involve utilizing the healthy dynamical modes as biomarkers to guide interventional strategies in the critically ill patients [56].

ACKNOWLEDGMENTS

The authors would like to acknowledge the comments of the anonymous reviewers of this manuscript. This work was supported by the National Institutes of Health (NIH) grant R01-EB001659, and R01GM104987, and by the NIH early career development award in biomedical big data science (1K01ES025445-01A1). The content of this article is solely the responsibility of the authors and does not necessarily represent the official views of the NIH.

REFERENCES

[1] A. Camm, M. Malik, J. Bigger, G. Breithardt, S. Cerutti, R. Cohen, P. Coumel, E. Fallen, H. Kennedy, R. Kleiger *et al.*, "Heart rate variability: standards of measurement, physiological interpretation and clinical use. Task Force of the European Society of Cardiology and the North American Society of Pacing and Electrophysiology," *Circulation*, vol. 93, no. 5, pp. 1043–1065, 1996.

[2] P. C. Ivanov, L. A. Amaral, A. L. Goldberger, S. Havlin, M. G. Rosenblum, Z. R. Struzik, and H. E. Stanley, "Multifractality in human heartbeat dynamics," *Nature*, vol. 399, pp. 461–5, 1999.

[3] M. Costa, A. L. Goldberger, and C. K. Peng, "Multiscale entropy analysis of complex physiologic time series," *Phys Rev Lett*, vol. 89, no. 6, p. 068102, 2002.

[4] S. Akselrod, D. Gordon, F. A. Ubel, D. C. Shannon, A. C. Berger, and R. J. Cohen, "Power spectrum analysis of heart rate fluctuation: a quantitative probe of beat-to-beat cardiovascular control." *Science*, vol. 213, no. 4504, pp. 220–222, Jul 1981.

[5] A. Malliani, M. Pagani, F. Lombardi, and S. Cerutti, "Cardiovascular neural regulation explored in the frequency domain." *Circulation*, vol. 84, no. 2, pp. 482–492, Aug 1991.

[6] N. Iyengar, C. K. Peng, R. Morin, A. L. Goldberger, and L. A. Lipsitz, "Age-related alterations in the fractal scaling of cardiac interbeat interval dynamics." *Am J Physiol*, vol. 271, no. 4, pp. R1078–R1084, Oct 1996.

[7] A. L. Goldberger, L. A. Amaral, J. M. Hausdorff, P. C. Ivanov, C.-K. Peng, and H. E. Stanley, "Fractal dynamics in physiology: alterations with disease and aging," *Proceedings of the National Academy of Sciences of the United States of America*, vol. 99, no. Suppl 1, pp. 2466–2472, 2002.

[8] M. Cohen and A. J. Taylor, "Short-term cardiovascular oscillations in man: measuring and modelling the physiologies," *Journal of Physiology*, vol. 542, no. Pt 3, pp. 669–683, 2002.

[9] A. Voss, S. Schulz, R. Schroeder, M. Baumert, and P. Caminal, "Methods derived from nonlinear dynamics for analysing heart rate variability," *Philosophical Transactions of the Royal Society A*, vol. 367, no. 1887, pp. 277–96, 2009.

[10] S. Schulz, F. C. Adochiei, I. R. Edu, R. Schroeder, H. Costin, K. Bär, and A. Voss, "Cardiovascular and cardiorespiratory coupling analyses: a review," *Philosophical Transactions of the Royal Society A*, vol. 371, no. 1997, p. 20120191, 2013.

[11] G. Parati, J. P. Saul, M. Di Rienzo, and G. Mancia, "Spectral analysis of blood pressure and heart rate variability in evaluating cardiovascular regulation a critical appraisal," *Hypertension*, vol. 25, no. 6, pp. 1276–1286, 1995.

[12] A. Mortara, P. Sleight, G. D. Pinna, R. Maestri, A. Prpa, M. T. La Rovere, F. Cobelli, and L. Tavazzi, "Abnormal awake respiratory patterns are common in chronic heart failure and may prevent evaluation of autonomic tone by measures of heart rate variability," *Circulation*, vol. 96, pp. 246–252, 1997.

[13] R. deBoer, J. Karemaker, and J. Strackee, "Relationships between short-term blood-pressure fluctuations and heart-rate variability in resting subjects I: a spectral analysis approach," *Med. & Biol. Eng. & Comput.*, vol. 23, pp. 352–358, 1985.

[14] G. Baselli, S. Cerutti, S. Civardi, D. Liberati, F. Lombardi, A. Malliani, and M. Pagani, "Spectral and cross-spectral analysis of heart rate and arterial blood pressure variability signals," *Computers and Biomedical Research*, vol. 19, pp. 520–534, 1986.

[15] L. Faes, G. Nollo, and K. Chon, "Assessment of granger causality by nonlinear model identification: application to short-term cardiovascular variability," *Ann Biomed Eng*, vol. 36, no. 3, pp. 381–95, 2008.

[16] M. Riedl, A. Suhrbier, H. Stepan, J. Kurths, and N. Wessel, "Short-term couplings of the cardiovascular system in pregnant women suffering from pre-eclampsia," *Philos Trans A Math Phys Eng Sci*, vol. 368, no. 1918, pp. 2237–50, 2010.

[17] R. Barbieri and E. N. Brown, "Application of dynamic point process models to cardiovascular control." *Biosystems*, vol. 93, no. 1-2, pp. 120–125, 2008.

[18] E. Gederi, S. Nemati, B. A. Edwards, G. D. Clifford, A. Malhotra, and A. Wellman, "Model-based estimation of loop gain using spontaneous breathing: A validation study," *Respiratory Physiology & Neurobiology*, vol. 201, pp. 84–92, 2014.

[19] L. H. Lehman, R. P. Adams, L. Mayaud, G. B. Moody, A. Malhotra, R. G. Mark, and S. Nemati, "A physiological time series dynamics-based approach to patient monitoring and outcome prediction," *IEEE Journal of Biomedical and Health Informatics*, vol. 19, no. 3, pp. 1068–1076, May 2015.

[20] S. Nemati, B. A. Edwards, S. A. Sands, P. J. Berger, A. Wellman, G. C. Verghese, A. Malhotra, and J. P. Butler, "Model-based characterization of ventilatory stability using spontaneous breathing," *J Appl Physiol*, vol. 111, no. 1, pp. 55–67, 2011.

[21] K. P. Murphy, "Switching Kalman filter," *Compaq Cambridge Research Laboratory, Tech. Rep. 98-10.*, 1998, Cambridge, MA.

[22] Y. Bar-Shalom and X. Li, *Estimation and Tracking: Principles, Techniques and Software*. Artech House, 1993.

[23] M. Saeed, M. Villarroel, A. T. Reisner, G. Clifford, L. H. Lehman, G. Moody, T. Heldt, T. H. Kyaw, B. Moody, and R. G. Mark, "Multiparameter intelligent monitoring in intensive care (MIMIC II): a public-access intensive care unit database." *Crit Care Med*, vol. 39, no. 5, pp. 952–960, May 2011.

[24] M. C. Khoo, "Modeling of autonomic control in sleep-disordered breathing," *Cardiovascular Engineering*, vol. 8, no. 1, pp. 30–41, 2008.

[25] R. Barbieri, G. Parati, and J. P. Saul, "Closed- versus open-loop assessment of heart rate baroreflex." *IEEE Eng Med Biol Mag*, vol. 20, no. 2, pp. 33–42, 2001.

[26] A. Goldberger, L. Amaral, L. Glass, J. Hausdorff, P. Ivanov, R. Mark, J. Mietus, G. Moody, C.-K. Peng, and H. Stanley, "PhysioBank, PhysioToolkit, and PhysioNet: Components of a new research resource for complex physiologic signals," *Circulation*, vol. 101, no. 23, pp. e215–e220, June 2000.

[27] T. Heldt, M. B. Oefinger, M. Hoshiyama, and R. G. Mark, "Circulatory response to passive and active changes in posture," *Computers in Cardiology*, vol. 30, pp. 263–266, 2003.

[28] S. Nemati, B. A. Edwards, J. Lee, B. Pittman-Polletta, J. P. Butler, and A. Malhotra, "Respiration and heart rate complexity: effects of age and gender assessed by band-limited transfer entropy." *Respir Physiol Neurobiol*, vol. 189, no. 1, pp. 27–33, Oct 2013.

[29] D. C. Angus, W. T. Linde-Zwirble, J. Lidicker, G. Clermont, J. Carcillo, and M. R. Pinsky, "Epidemiology of severe sepsis in the united states: analysis of incidence, outcome, and associated costs of care." *Crit Care Med*, vol. 29, no. 7, pp. 1303–1310, Jul 2001.

[30] R. P. Dellinger, M. M. Levy, J. M. Carlet *et al.*, "Surviving sepsis campaign: International guidelines for management of severe sepsis and septic shock: 2008," *Intensive Care Medicine*, vol. 34, pp. 17–60, 2008.

[31] G. Schwarz, "Estimating the dimension of a model," *Annals of Statistics*, vol. 6, no. 2, pp. 461–464, 1978.

[32] Y. Benjamini and H. Y., "Controlling the false discovery rate: a practical and powerful approach to multiple testing," *Journal of the Royal Statistical Society*, vol. 57, no. 1, pp. 289–300, 1995.

[33] W. A. Knaus, D. P. Wagner, E. A. Draper, J. E. Zimmerman, M. Bergner, P. G. Bastos, C. A. Sirio, D. J. Murphy, T. Lotring, A. Damiano, and F. Harrell, "The APACHE III prognostic system," *Chest*, vol. 100, 1991.

[34] E. R. DeLong, D. M. DeLong, and D. L. Clarke-Pearson, "Comparing the areas under two or more correlated receiver operating characteristic curves: a nonparametric approach," *Biometrics*, pp. 837–845, 1988.

[35] J. P. Saul, R. D. Berger, M. H. Chen, and R. J. Cohen, "Transfer function analysis of autonomic regulation. II. respiratory sinus arrhythmia," *Am J Physiol*, vol. 256, no. 1 Pt 2, pp. H153–H161, Jan 1989.

[36] Z. Chen, E. N. Brown, and R. Barbieri, "Assessment of autonomic control and respiratory sinus arrhythmia using point process models of human heart beat dynamics." *IEEE Trans Biomed Eng*, vol. 56, no. 7, pp. 1791–1802, Jul 2009.

[37] X. Xiao, T. J. Mullen, and R. Mukkamala, "System identification: a multi-signal approach for probing neural cardiovascular regulation." *Physiol Meas*, vol. 26, no. 3, pp. R41–R71, Jun 2005.

[38] D. M. Kaye and M. D. Esler, "Autonomic control of the aging heart," *Neuromolecular medicine*, vol. 10, no. 3, pp. 179–186, 2008.

[39] J. Wizorek and T. Buchman, "Organ-organ interactions in multiple organ failure," in *Mechanisms of Oran Dysfunction in Critical Illness*. Springer-Verlag, 2002.

[40] H. Schmidt, U. Mller-Werdan, T. Hoffmann, D. P. Francis, M. F. Piepoli, M. Rauchhaus, R. Prondzinsky, H. Loppnow, M. Buerke, D. Hoyer, and K. Werdan, "Autonomic dysfunction predicts mortality in patients with multiple organ dysfunction syndrome of different age groups." *Crit Care Med*, vol. 33, no. 9, pp. 1994–2002, Sep 2005.

[41] J. Scheff, P. Mavroudis, S. Calvano, S. Lowry, and I. Androulakis, "Modeling autonomic regulation of cardiac function and heart rate variability in human endotoxemia." *Physiological genomics*, vol. 43, no. 16, pp. 951–64, 2011.

[42] S. M. Pincus and A. L. Goldberger, "Physiological time-series analysis: What does regularity quantify?" *American Journal of Physiology*, vol. 266, no. 4 Pt 2, pp. H1643–56, 1994.

[43] P. J. Godin and T. G. Buchman, "Uncoupling of biological oscillators: a complementary hypothesis concerning the pathogenesis of multiple organ dysfunction syndrome." *Crit Care Med*, vol. 24, no. 7, pp. 1107–1116, Jul 1996.

[44] L. A. Fleisher, S. M. Frank, D. I. Sessler, C. Cheng, T. Matsukawa, and C. A. Vannier, "Thermoregulation and heart rate variability," *Clinical Science*, vol. 90, no. 2, pp. 97–103, 1996.

[45] M. P. Griffin, D. E. Lake, T. M. O'Shea, and J. R. Moorman, "Heart rate characteristics and clinical signs in neonatal sepsis." *Pediatr Res*, vol. 61, no. 2, pp. 222–227, Feb 2007.

[46] S. Ahmad, T. Ramsay, L. Huebsch, S. Flanagan, S. McDiarmid, I. Batkin, L. McIntyre, S. R. Sundaresan, D. E. Maziak, F. M. Shamji *et al.*, "Continuous multi-parameter heart rate variability analysis heralds onset of sepsis in adults," *PLoS One*, vol. 4, no. 8, p. e6642, 2009.

[47] S. Saria, A. K. Rajani, J. Gould, D. Koller, and A. Penn, "Integration of early physiological responses predicts later illnessseverity in preterm infants," *Science Translational Medicine*, vol. 2, no. 48, pp. 48–65, 2010.

[48] J. A. Quinn, C. K. Williams, and N. McIntosh, "Factorial switching linear dynamical systems applied to physiological condition monitoring," *IEEE Transactions on Pattern Analysis and Machine Intelligence*, vol. 31, no. 9, pp. 1537–1551, 2009.

[49] I. Stanculescu, C. K. Williams, and Y. Freer, "Autoregressive Hidden Markov Models for the Early Detection of Neonatal Sepsis," *IEEE Journal of Biomedical and Health Informatics*, pp. 1560–1570, 2014.

[50] L. H. Lehman, M. Johnson, S. Nemati, R. P. Adams, and R. G. Mark, "Bayesian nonparametric learning of switching dynamics in cohort physiological time series: application in critical care patient monitoring," in *Advanced State Space Methods for Neural and Clinical Data*, Z. Chen, Ed. Cambridge University Press, 2015, pp. 257–282.

[51] L. T. Mainardi, A. M. Bianchi, R. Furlan, S. Piazza, R. Barbieri, V. di Virgilio, A. Malliani, and S. Cerutti, "Multivariate time-variant identification of cardiovascular variability signals: a beat-to-beat spectral parameter estimation in vasovagal syncope." *IEEE Trans Biomed Eng*, vol. 44, no. 10, pp. 978–989, Oct 1997.

[52] M. Leone, P. Asfar, P. Radermacher, J. L. Vincent, and C. Martin, "Optimizing mean arterial pressure in septic shock: a critical reappraisal of the literature," *Crit Care*, vol. 19, p. 101, 2015.

[53] R. Kato and M. R. Pinsky, "Personalizing blood pressure management in septic shock," *Annals of intensive care*, vol. 5, no. 1, pp. 1–10, 2015.

[54] G. Parati, J. E. Ochoa, C. Lombardi, and G. Bilo, "Assessment and management of blood-pressure variability." *Nat Rev Cardiol*, vol. 10, no. 3, pp. 143–155, Mar 2013.

[55] L. H. Lehman, S. Nemati, and R. G. Mark, "Hemodynamic monitoring using switching autoregressive dynamics of multivariate vital sign time series," in *Proceedings of the Computing in Cardiology*, 2015, pp. 1065–1068.

[56] W. D. Schweickert and J. P. Kress, "Strategies to optimize analgesia and sedation," *Critical Care*, vol. 12, no. Suppl 3, p. S6, 2008.

APPENDIX

A: Association Analysis of Individual Dynamic Modes and Severe Sepsis

Mode	P	OR(95%CI)	P_{adj}	Adj OR(95%CI)	HL P
2	**0.0000**	1.95(1.59, 2.40)	**0.0001**	1.64(1.28,2.11)	0.25
9	**0.0001**	0.19(0.08, 0.44)	**0.0022**	0.23(0.09,0.59)	0.35
5	**0.0017**	0.35(0.19, 0.68)	**0.0095**	0.34(0.15,0.77)	0.42
4	0.0032	2.26(1.31, 3.90)	0.3311	1.46(0.68, 3.12)	0.24
8	0.0048	0.41(0.22, 0.76)	0.3645	0.71(0.34, 1.49)	0.16
1	0.1953	0.88(0.72, 1.07)	0.7630	1.04(0.79, 1.38)	0.29
3	0.2146	1.19(0.90, 1.58)	0.3465	1.19(0.83, 1.69)	0.29
10	0.4948	0.90(0.66, 1.22)	0.2009	0.78(0.53, 1.14)	0.21
7	0.5116	0.84(0.51, 1.40)	0.9839	1.01(0.55, 1.85)	0.30
6	0.6159	0.91(0.62, 1.33)	0.3118	0.77(0.46, 1.28)	0.33

TABLE VI
ASSOCIATIONS BETWEEN THE DURATION OF TIME (MEASURED AS MODE PROPORTIONS) PATIENTS SPENT IN EACH OF THE TEN MOST COMMON HR/MAP DYNAMIC MODES AND THE ODDS OF SEVERE SEPSIS. HL P - P VALUE FROM HOSMER LEMESHOW.

Table VI summarizes the association analysis of the mode proportion in each of the top ten most common bivariate HR/BP dynamic modes and severe sepsis. We built a separate univariable/multivariable logistic regression model for each of the top ten most common dynamic modes. In the multivariable logistic regression model, we report the adjusted P values and ORs of the dynamic mode proportion variables after adjusting for clinical interventions and patients' severity of illness as measured by their APACHE-III scores.